

Observation of the Exotic 0_2^+ Cluster State in ${}^8\text{He}$

Z. H. Yang^{1,2,*}, Y. L. Ye^{1,*}, B. Zhou^{3,4,5}, H. Baba², R. J. Chen⁶, Y. C. Ge¹, B. S. Hu¹, H. Hua¹, D. X. Jiang¹, M. Kimura^{2,5,7}, C. Li², K. A. Li⁶, J. G. Li¹, Q. T. Li¹, X. Q. Li¹, Z. H. Li¹, J. L. Lou¹, M. Nishimura², H. Otsu², D. Y. Pang⁸, W. L. Pu¹, R. Qiao¹, S. Sakaguchi^{2,9}, H. Sakurai², Y. Satou¹⁰, Y. Togano², K. Tshoo¹⁰, H. Wang^{2,11}, S. Wang², K. Wei¹, J. Xiao¹, F. R. Xu¹, X. F. Yang¹, K. Yoneda², H. B. You¹ and T. Zheng¹

¹School of Physics and State Key Laboratory of Nuclear Physics and Technology, Peking University, Beijing 100871, China

²RIKEN Nishina Center, 2-1 Hirosawa, Wako, Saitama 351-0198, Japan

³Key Laboratory of Nuclear Physics and Ion-beam Application (MOE), Institute of Modern Physics, Fudan University, Shanghai 200433, China

⁴Shanghai Research Center for Theoretical Nuclear Physics, NSFC and Fudan University, Shanghai 200438, China

⁵Department of Physics, Hokkaido University, 060-0810 Sapporo, Japan

⁶Institute of Modern Physics, Chinese Academy of Science, Lanzhou 730000, China


⁷Nuclear Reaction Data Centre, Hokkaido University, 060-0810 Sapporo, Japan

⁸School of Physics and Beijing Key Laboratory of Advanced Nuclear Materials and Physics, Beihang University, Beijing 100191, China

⁹Department of Physics, Kyushu University, 819-0395 Fukuoka, Japan

¹⁰Rare Isotope Science Project, Institute for Basic Science, Daejeon 34000, Republic of Korea

¹¹Department of Physics, Tokyo Institute of Technology, 2-12-1 Oh-Okayama, Meguro, Tokyo 152-8551, Japan

 (Received 17 April 2023; revised 5 September 2023; accepted 1 November 2023; published 13 December 2023)

We report here the first observation of the 0_2^+ state of ${}^8\text{He}$, which has been predicted to feature the condensatelike $\alpha + {}^2n + {}^2n$ cluster structure. We show that this state is characterized by a spin parity of 0^+ , a large isoscalar monopole transition strength, and the emission of a strongly correlated neutron pair, in line with theoretical predictions. Our finding is further supported by the state-of-the-art microscopic $\alpha + 4n$ model calculations. The present results may lead to new insights into clustering in neutron-rich nuclear systems and the pair correlation and condensation in quantum many-body systems under strong interactions.

DOI: [10.1103/PhysRevLett.131.242501](https://doi.org/10.1103/PhysRevLett.131.242501)

Introduction.—The quantum condensate is a novel state of matter predicted by Bose and Einstein, and initially observed in 1995 by Cornell, Wieman, and Ketterle in a gas of ultracold bosonic atoms [1,2]. Despite the Pauli exclusion principle, the condensation in a system of fermionic atoms can also be realized by forming either bound diatomic molecules or correlated atom pairs [3–5]. The nuclear analog, a condensation of strongly correlated spin-singlet neutron pairs in nuclear matter or in finite nuclei, has been theoretically predicted [6–10] and suggested to be essential for the cooling process of neutron stars and glitches of pulsars [11,12], but its experimental observation has remained elusive. In the context of condensation in nuclear systems, evidence has been accumulated in recent years for the Bose-Einstein condensation of α particles [13–16]. The most well-known example is the Hoyle state of ${}^{12}\text{C}$ with a 3α -condensatelike cluster structure, which is the key for the nucleosynthesis of carbon in stars and thereby crucial for carbon-based life including the human [14–17].

The occurrence of one single 2n [dineutron, a compact spin-singlet ($S = 0$) neutron pair in internal orbital s wave] has been intensively investigated in neutron-rich nuclei

close to the boundary of the nuclear chart (the neutron drip line) [18–21]. Recently, the 2n cluster was also suggested to be an essential ingredient in the structure of four-neutron systems [22,23]. When it comes to the 2n -condensate state, the simplest case would be the core-plus- $4n$ nuclei such as ${}^8\text{He}$, since 2n should be enhanced at the diffused surface of such neutron-rich nuclei [18,21,24]. Particularly, recent theoretical studies using the *ab initio*-type antisymmetrized molecular dynamics (AMD) model [9] and the 2n cluster model [10] predicted a condensatelike $\alpha + {}^2n + {}^2n$ cluster structure in the 0_2^+ state of ${}^8\text{He}$, closely resembling the 3α -condensatelike structure of the Hoyle state [14–17]. The essential features of this cluster state are the expanded distribution of 2n clusters in relative s waves and a large isoscalar monopole transition strength [10]. However, it has remained an experimental challenge to populate and identify such well clustered multineutron systems, which requires the availability of high-intensity ${}^8\text{He}$ beams at moderate energies, precise detection of the multiple decay neutrons, and identification of the condensatelike cluster state from experimental observables.

In this Letter, we report on the observation of a new excited state of ${}^8\text{He}$. By analyzing the differential cross

sections, we have determined its spin parity to be 0^+ and also extracted its characteristic transition strength. These findings signal a condensatelike $\alpha + {}^2n + {}^2n$ cluster structure in ${}^8\text{He}$, which is further supported by the state-of-the-art $\alpha + 4n$ model calculations.

Experiment.—The experiment was carried out at the RIPS beam line of RIKEN Nishina Center [25], which provides the high-intensity ${}^8\text{He}$ beam ($>10^5$ pps) at an energy of 82.3 MeV/nucleon. The beam particles were identified with the TOF- ΔE method using two plastic scintillators on the beam line. Their trajectories were measured by two drift chambers placed upstream of the target. We have carried out combined measurements with a $(\text{CH}_2)_n$ target (polyethylene foil, 83 mg/cm²), and a carbon target (133.9 mg/cm²) to compare reactions with carbon and hydrogen nuclei, together with an empty target for the background measurement. The charged fragments were deflected by a dipole magnet, and their trajectories and TOF were measured by two drift chambers and a plastic scintillator array respectively. A neutron detector array, consisting of 60 plastic scintillator modules arranged into four separated layers, was installed at 4.5 meter downstream of the target to measure the beam-velocity neutrons, with a time resolution (σ) of ~ 400 ps. To remove the γ ray background, an energy threshold of 6 MeVee (electron equivalent) was imposed. More details of the experimental setup and detector performance can be found in our previous papers using the same setup [26–28] and a schematic can be found in [29].

Resonant states of ${}^8\text{He}$ were populated via inelastic excitation, and their decay energies (E_r), with respect to the ${}^6\text{He} + 2n$ threshold ($S_{2n} = 2.12$ MeV), are reconstructed from momenta of the ${}^6\text{He}$ fragment and the two decay neutrons. The criterion to reject misidentified $2n$ events (so-called “crosstalks”) is optimized using GEANT4 simulations considering the realistic experimental setup [27,31–33]. For events with two hits in the same layer or two closely packed layers, the crosstalk is identified from the small distance between the two hits ($\Delta x \leq 200$ mm and $\Delta y \leq 200$ mm). For events with two hits in two well separated layers, their kinematical correlation is considered. A rejection ratio of $>99\%$ is achieved, as verified using data of the single-neutron-emission reaction ${}^7\text{Li}(p, n){}^7\text{Be}$ [27], and the residual crosstalk is estimated to be less than 5% in the observed $2n$ events (see Fig. S3 in [29]). The efficiency is $\sim 19\%$ for $1n$ events and $\sim 4\%$ for $2n$ events at $E_r = 1$ MeV, and decreases with E_r due to loss of acceptance. In the E_r range around the peak of the ${}^8\text{He}(0_2^+)$ state (4–5 MeV, see below), the resolution (σ) for E_r is ~ 0.25 MeV, and the efficiency (detecting ${}^6\text{He}$ and $2n$ in coincidence) is $\sim 0.7\%$.

Background exclusion through angular correlation analysis.—Population of cluster states like ${}^8\text{He}(0_2^+)$ and the subsequent neutron emission may be accompanied by some other processes without forming a resonant state

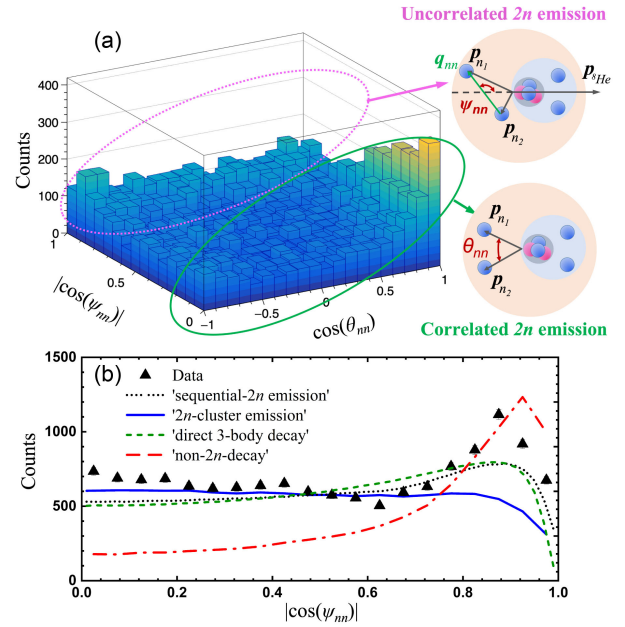


FIG. 1. (a) Correlated plot between $\cos(\theta_{nn})$ and $|\cos(\psi_{nn})|$, exhibiting distinct behaviors in the small- and large- $|\cos(\psi_{nn})|$ regions. (b) $|\cos(\psi_{nn})|$ spectrum compared to simulations of different $2n$ -emission processes (details in text).

(hereafter referred to as “non- $2n$ -decay” process) [34–37]. To identify and thus reject such non- $2n$ -decay events, we developed a method based on correlated analysis of the n - n opening angle θ_{nn} and the opening angle ψ_{nn} between the n - n relative momentum \mathbf{q}_{nn} and the momentum vector (laboratory frame) of ${}^8\text{He}$ $\mathbf{P}_{{}^8\text{He}}$.

As shown in Fig. 1(a), the $\cos(\theta_{nn}) - \cos(\psi_{nn})$ correlated plot exhibits distinct behaviors in the small- and large- $|\cos(\psi_{nn})|$ regions (marked by the green-solid and pink-dotted ovals). Apparently, the small- $|\cos(\psi_{nn})|$ region is characterized by enhancement at $\cos(\theta_{nn}) \sim 1$ (equivalently, $\theta_{nn} \sim 0$), indicating significant correlations between the two neutrons. The large- $|\cos(\psi_{nn})|$ region, on the other hand, shows basically a flat $\cos(\theta_{nn})$ distribution, indicating most likely uncorrelated $2n$ emission.

In Fig. 1(b), the inclusive $|\cos(\psi_{nn})|$ spectrum is compared to simulations of different $2n$ -emission processes. In principal, for $2n$ emission from ${}^8\text{He}$ resonant states, the $|\cos(\psi_{nn})|$ spectrum should exhibit a uniform distribution (except the effects of experimental acceptance) regardless of the specific decay process. This is consistent with our simulations assuming three different decay processes: (1) emission of a strongly correlated neutron pair in s wave that is modeled using the n - n scattering length [7,19,38] (“ $2n$ -cluster emission,” shown as the blue-solid line); (2) “sequential- $2n$ emission” (gray-dotted line) via the intermediate ${}^7\text{He}$ ground state (g.s) with the energy and width taken from our previous publication [26], and (3) “direct three-body decay” (green-dashed line) governed solely by the three-body phase space in the final state.

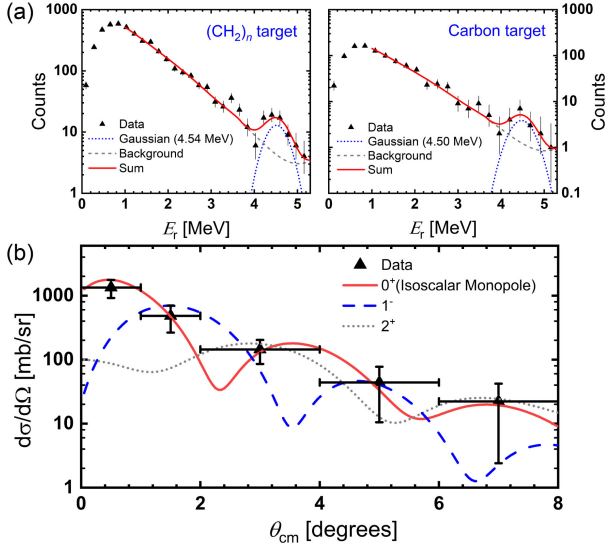


FIG. 2. (a) E_r spectra for $(\text{CH}_2)_n$ and carbon targets (c.m. scattering angle $\theta_{\text{c.m.}} < 2^\circ$), fitted using a Gaussian peak and a second-order polynomial background, modified by the acceptance. Error bars are statistical only (1 s.d.). Negligible contribution from the target frame was checked with the empty target data. (b) Angular distribution of the 4.5-MeV state for the $(\text{CH}_2)_n$ target. Horizontal error bars stand for the bin size and vertical ones for the combined statistical and systematic uncertainties. The curves show the least-square fitting with DWBA calculations convoluted with the resolution ($\sigma = 0.2^\circ$). A spin parity of 0^+ is clearly supported due to the much smaller χ^2 (0.9) compared to 1^- (11.4) and 2^+ (13.6).

The sharp increase toward $|\cos(\psi_{nn})| \sim 1$ can only be explained by non- $2n$ -decay (red-dash-dotted line) where one of the two neutrons is strongly affected by the target without forming resonant states. Indeed, we find the E_r spectrum gated by $|\cos(\psi_{nn})| > 0.65$ (Fig. S4 in Supplemental Material [29]) is mainly structureless continuum. Therefore, in the analysis below only events within $|\cos(\psi_{nn})| < 0.65$ are used, and the effect of this cut on our results has been checked by varying the cutoff value.

Identification of the 0_2^+ resonant state.—As shown in Fig. 2(a), we first analyzed the E_r spectrum at very forward angles (the c.m. scattering angle $\theta_{\text{c.m.}} < 2^\circ$) for both $(\text{CH}_2)_n$ and carbon targets, where the monopole transition from ${}^8\text{He}(\text{g.s.})$ to ${}^8\text{He}(0_2^+)$ should be enhanced [39]. A prominent peak at 4.54(6) MeV is clearly observed for the $(\text{CH}_2)_n$ target, with a significance level larger than 5σ . We have checked that this peak is stable under variations of the applied $|\cos(\psi_{nn})|$ cut. We further checked the E_r spectra for different $\theta_{\text{c.m.}}$ bins; in all cases the prominent peak at ~ 4.5 MeV is clearly identified (Fig. S2 in [29]), firmly evidencing the observation of this state. Similarly, for the carbon target a statistically significant peak is observed at 4.50(20) MeV. The cross sections for $(\text{CH}_2)_n$ and carbon targets in the peak region are approximately the same, indicating the predominant role of isospin-saturated carbon

nuclei in populating this state. We indeed find this state is basically absent when subtracting the carbon contribution from the $(\text{CH}_2)_n$ -target spectrum, consistent with experiments using proton target ([40] and references therein). Similar behavior was also observed for the Hoyle state with a 3α -condensate cluster structure—the population cross section for the proton target is more than ten times smaller than that for the isospin-saturated ${}^4\text{He}$ target [41].

The differential cross section for each angular bin was then extracted according to the corresponding Gaussian peak counting (Fig. S2 in [29]). Note that a small portion of events belonging to this resonant state will also be rejected by $|\cos(\psi_{nn})| < 0.65$, but this can be corrected by using the simulated $|\cos(\psi_{nn})|$ spectrum as mentioned above. In Fig. 2(b), the data are compared to distorted-wave born approximation (DWBA) calculations that were carried out using FRESKO [42] with the optical potential taken from ${}^8\text{He} + {}^{12}\text{C}$ elastic scattering at a similar energy [43]. For the isoscalar (IS) monopole transition with the transferred angular momentum $L = 0$, the form factor was modeled with the breathing-mode oscillation [39,44]. The transition with $L = 1$ (Harakeh-Dieperink form factor [45]) and $L = 2$ (Bohr-Mottelson form factor [46]) were also calculated. This comparison supports a spin-parity assignment of 0^+ , meanwhile clearly ruling out other possibilities. This is the first observation of a low-lying 0^+ excited state in ${}^8\text{He}$, thanks to the above described exclusion of the non- $2n$ -decay background. At energies lower than this 0^+ resonance, some other states, such as the intensively studied 2^+ state and candidate 1^+ state, should have been populated but imbedded in the continuum [40,47–49]. There might be another state at $E_r \sim 3.5$ MeV, but its existence could not be firmly established due to the limited statistics.

IS monopole transition strength.—The IS monopole transition strength, denoted by the corresponding transition matrix element $M(\text{IS0})$, has proven to be a sensitive probe for cluster formation in excited states of light nuclei [39,50,51]. An abnormally large $M(\text{IS0})$ for low-lying 0^+ excited states ($\lesssim 10$ MeV), comparable to or higher than the respective single-particle transition strength (~ 5 fm 2), cannot be explained within the single-particle picture, and should instead be the fingerprint of distinctive cluster structures [39,50,51]. The method to extract $M(\text{IS0})$ from the differential cross sections has been well established in our previous work [39,44]. The DWBA calculation was performed for an IS monopole transition with a strength corresponding to the energy-weighted sum rule $S(\text{IS0}) = (2\hbar^2/m)AR_{\text{rms}}^2$, defined by the mass number A and the matter radius R_{rms} [39,52]. For ${}^8\text{He}$, $A = 8$ and $R_{\text{rms}} = 2.52(3)$ fm [53]. By normalizing the calculated cross sections to our data as indicated by the red-solid line in Fig. 2(b), $M(\text{IS0}) = 11_{-2.3}^{+1.8}$ fm 2 was deduced. Here, the uncertainty combines the statistical (1.2 fm 2) and systematic ($_{-2.0}^{+1.3}$ fm 2) uncertainties. Our result is in excellent

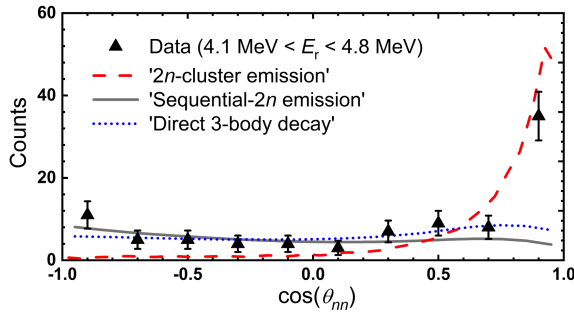


FIG. 3. $\cos(\theta_{nn})$ spectrum of ${}^8\text{He}(0_2^+)$, compared to simulations of different decay models (details in text). The gates $|\cos(\psi_{nn})| < 0.65$ and $\theta_{c.m.} < 2^\circ$ are applied to reduce the background. Error bars are statistical only (1 s.d.).

agreement with the predicted value of 9.0 fm^2 , associated with a condensatelike $\alpha + {}^2n + {}^2n$ cluster structure [10].

We note that ${}^8\text{He}(0_2^+)$ decays predominantly into the ${}^6\text{He} + 2n$ channel while the ${}^4\text{He} + 4n$ channel is negligible due to the much smaller phase space. Therefore, the $M(\text{ISO})$ obtained here from the ${}^6\text{He} + 2n$ channel is approximately equal to the overall transition strength.

Emission of strongly correlated two neutrons.—A 2n -condensate state in neutron-rich nuclei contains two or more 2n clusters all moving in s wave relative to the core [9,10]. Here, we use l_y and l_x to denote the orbital angular momentum between the c.m. of the 2n and the core and that between the two neutrons of 2n [38,54,55]. In the current experiment measuring the decay of ${}^8\text{He}(0_2^+)$ into ${}^6\text{He}(\text{g.s.}) + 2n$, given that ${}^6\text{He}(\text{g.s.})$ is dominated by the $\alpha + {}^2n$ structure with $l_y = 0$ [54,56], the determination of $l_x = 0$ for the emitted neutron pair would thus lead to $S = l_y = 0$ due to the antisymmetrization and the total angular momentum conservation [9,10].

In Fig. 3, the $\cos(\theta_{nn})$ spectrum of ${}^8\text{He}(0_2^+)$ is compared to simulations. Obviously, sequential- $2n$ emission (gray-solid line) and direct three-body decay (blue-dotted line)—without n - n correlations—give a rather flat distribution. In contrast, $2n$ -cluster emission (red-dashed line) reproduces well the characteristic increase at $\cos(\theta_{nn}) \sim 1.0$. This analysis indicates the strong correlation between the two decay neutrons that is consistent with emission of a neutron pair having $l_x = 0$ from a resonant state well above the neutron-emission threshold (see also Fig. 2 of [38]). We note that several decay models incorporating the full three-body final state interactions are under development [38,47,55,57] and the $2n$ correlation data of ${}^8\text{He}(0_2^+)$ could help to test their calculations.

Theoretical calculations and discussions.—In addition to the above noted cluster model [10] and AMD [9] calculations, a low-lying ${}^8\text{He}(0_2^+)$ state was also predicted by the *ab initio* quantum Monte Carlo calculation [58], with an excitation energy ($\sim 7 \text{ MeV}$) close to our data $6.66(6) \text{ MeV}$. To unravel the condensatelike $\alpha + {}^2n + {}^2n$ cluster structure,

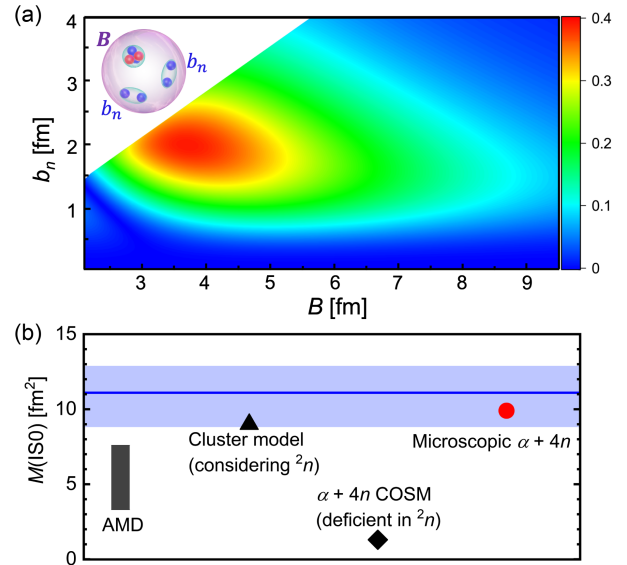


FIG. 4. (a) Overlap of the ${}^8\text{He}(0_2^+)$ wave function with the 2n -condensate THSR wave functions $\Phi(\mathbf{B}, b_n)$ specified by B and b_n (illustration in the inset). The cutoff in the upper left corner originates from the forbidden states of $\Phi(\mathbf{B}, b_n)$. (b) $M(\text{ISO})$ of ${}^8\text{He}(0_2^+)$. Our data are presented as the blue-solid line with a shaded band showing the combined statistical and systematic uncertainty, and compared to calculations of COSM [62], AMD [9], the 2n cluster model [10], and our microscopic $\alpha + 4n$ model.

we first performed microscopic calculations by employing the Tohsaki-Horiuchi-Schuck-Röpke (THSR) wave function, which has been proven to be an essential tool to describe the α -condensate cluster states such as the well-known Hoyle state [13–15,59,60]. Here, we consider a specific $\alpha + {}^2n + {}^2n$ cluster structure of condensation character—one α cluster of size b_α and two identical 2n clusters of size b_n moving in the lowest s -wave orbit in a “container” of size B [61] [inset of Fig. 4(a)]. The intrinsic THSR wave function is expressed as

$$\Phi(\mathbf{B}, b_n) \propto \mathcal{A} \left\{ \exp \left[-\frac{4\xi_1^2}{3B^2} - \frac{3\xi_2^2}{2B^2} \right] \times \phi_\alpha(b_\alpha) \phi_{{}^2n}(b_n) \phi_{{}^2n}(b_n) \right\}, \quad (1)$$

with ξ_1 and ξ_2 being the intercluster Jacobi coordinates defined in terms of the c.m. coordinates ($\mathbf{X}_\alpha, \mathbf{X}_{n1}, \mathbf{X}_{n2}$) of α and two 2n clusters: $\xi_1 = \mathbf{X}_\alpha - \mathbf{X}_{n1}$, $\xi_2 = \mathbf{X}_{n2} - (4\mathbf{X}_\alpha + 2\mathbf{X}_{n1})/6$. ϕ_α and $\phi_{{}^2n}$ are their intrinsic wave functions. Using the same nuclear interaction as [10], a low-lying 0_2^+ state was indeed found at 4.5 MeV above the $\alpha + 4n$ threshold, close to the experimental value of $3.52(6) \text{ MeV}$. The THSR calculation thus supports the 2n -condensate cluster structure as the essential ingredient of this newly observed ${}^8\text{He}(0_2^+)$ state.

To gain further insight into the 2n -condensate cluster structure, we then resort to microscopic $\alpha + 4n$ model calculations without assuming preformation of 2n clusters. The previous five-body $\alpha + 4n$ calculation with the cluster orbital shell model (COSM) was deficient in the neutron correlation and predicted a predominant single-particle structure for ${}^8\text{He}(0_2^+)$ [62]. In our microscopic $\alpha + 4n$ model, we have fully accounted for the formation and breakup of 2n clusters out of the four valence neutrons, which allows the condensatelike $\alpha + {}^2n + {}^2n$ cluster structure to naturally arise (more details in [29]). The same nuclear interactions as [10] (termed as “m55”) are used, and 0_2^+ is found at 4.4 MeV above the $\alpha + 4n$ threshold, consistent with [9,10]. Similar to [10], we examine the 2n -condensate cluster structure by computing the overlap of ${}^8\text{He}(0_2^+)$ with the 2n -condensate configurations described by the above THSR wave function and specified by the size parameters b_n and B . As visualized in Fig. 4(a), compact dineutron clusters ($b_n \sim 2$ fm) and their dilute-gas-like motion characterized by the broad distribution of B are readily apparent, as expected for a 2n -condensate cluster structure [10]. In contrast to the previous five-body $\alpha + 4n$ calculation [62], the currently calculated large $M(\text{ISO})$ of 9.9 fm^2 also agrees excellently with our observed value of $11.1_{-2.3}^{+1.8} \text{ fm}^2$ [Fig. 4(b)], providing further compelling evidence for the 2n -condensate cluster structure in ${}^8\text{He}(0_2^+)$. We have also made calculations using different nuclear interactions, finding that the variation of the predicted $M(\text{ISO})$ is within 1 fm^2 .

Summary.—For the first time we have observed the 0_2^+ state of ${}^8\text{He}$, which was predicted to exhibit a condensate-like $\alpha + {}^2n + {}^2n$ structure. This state is characterized by a large isoscalar monopole transition strength and the emission of a strongly correlated neutron pair, in line with theoretical predictions. State-of-the-art $\alpha + 4n$ model calculation further supports the correspondence between the observed properties of this state and the condensatelike cluster structure. This finding unveils a new distinctive property of neutron-rich systems which may have significant implications for understanding the properties of neutron stars. We anticipate such measurements being extended to more neutron-rich nuclei around the neutron drip line, taking advantages of the operating and upcoming radioactive ion-beam facilities worldwide.

We thank the RIKEN Nishina Center accelerator staff and RIPS team for providing the high-quality beams. We thank Y. Funaki, M. N. Harakeh, H. Horiuchi, Y. Kanada-En’yo, Z. Kohley, Y. Kondo, T. Myo, H. J. Ong, A. Tohsaki, and S. M. Wang for discussions. This work was supported by the National Key R&D Program of China (Grants No. 2022YFA1605100, No. 2023YFE0101500, No. 2023YFE0101600), the National Natural Science Foundation of China (Grants

No. 12027809, No. 12275006, No. 11961141003, No. U1967201, No. 12175042, No. 12335007), and the JSPS KAKENHI Grants of Japan No. 17K14262 [Grant-in-Aid for Young Scientists (B)], the State Key Laboratory of Nuclear Physics and Technology, Peking University (No. NPT2022ZZ02). Numerical computations were performed at the Yukawa Institute Computer Facility in Kyoto University. We also thank Z. X. Cao, L. H. Lv, S. Deguchi, Y. Kondo, and Y. Nakayama for their support during the experiment.

*These authors have contributed equally to this work.

†zaihong.yang@pku.edu.cn

‡yeyl@pku.edu.cn

- [1] M. H. Anderson, J. R. Ensher, M. R. Matthews, C. E. Wieman, and E. A. Cornell, *Science* **269**, 198 (1995).
- [2] K. B. Davis, M. O. Mewes, M. R. Andrews, N. J. van Druten, D. S. Durfee, D. M. Kurn, and W. Ketterle, *Phys. Rev. Lett.* **75**, 3969 (1995).
- [3] M. Greiner, C. A. Regal, and D. S. Jin, *Nature (London)* **426**, 537 (2003).
- [4] C. A. Regal, M. Greiner, and D. S. Jin, *Phys. Rev. Lett.* **92**, 040403 (2004).
- [5] M. W. Zwierlein, J. R. Abo-Shaeer, A. Schirotzek, C. H. Schunck, and W. Ketterle, *Nature (London)* **435**, 1047 (2005).
- [6] J. Xiao, Y. L. Ye, H. B. You, Z. H. Yang, and Y. L. Sun, *Nucl. Phys. Rev.* **29**, 317 (2012).
- [7] M. Matsuo, *Phys. Rev. C* **73**, 044309 (2006).
- [8] A. Sedrakian and J. W. Clark, *Eur. Phys. J. A* **55**, 167 (2019).
- [9] Y. Kanada-En’yo, *Phys. Rev. C* **76**, 044323 (2007).
- [10] F. Kobayashi and Y. Kanada-En’yo, *Phys. Rev. C* **88**, 034321 (2013).
- [11] D. Page, M. Prakash, J. M. Lattimer, and A. W. Steiner, *Phys. Rev. Lett.* **106**, 081101 (2011).
- [12] G. Watanabe and C. J. Pethick, *Phys. Rev. Lett.* **119**, 062701 (2017).
- [13] A. Tohsaki, H. Horiuchi, P. Schuck, and G. Röpke, *Phys. Rev. Lett.* **87**, 192501 (2001).
- [14] A. Tohsaki, H. Horiuchi, P. Schuck, and G. Röpke, *Rev. Mod. Phys.* **89**, 011002 (2017).
- [15] P. Schuck, Y. Funaki, H. Horiuchi, G. Röpke, A. Tohsaki, and T. Yamada, *Phys. Scr.* **91**, 123001 (2016).
- [16] S. Adachi, Y. Fujikawa, T. Kawabata, H. Akimune, T. Doi *et al.*, *Phys. Lett. B* **819**, 136411 (2021).
- [17] M. Freer and H. Fynbo, *Prog. Part. Nucl. Phys.* **78**, 1 (2014).
- [18] K. Hagino, H. Sagawa, J. Carbonell, and P. Schuck, *Phys. Rev. Lett.* **99**, 022506 (2007).
- [19] A. Spyrou, Z. Kohley, T. Baumann, D. Bazin, B. A. Brown, G. Christian *et al.*, *Phys. Rev. Lett.* **108**, 102501 (2012).
- [20] T. Nakamura, A. M. Vinodkumar, T. Sugimoto, N. Aoi, H. Baba, D. Bazin *et al.*, *Phys. Rev. Lett.* **96**, 252502 (2006).
- [21] Y. Kubota, A. Corsi, G. Authalet, H. Baba, C. Caesar *et al.*, *Phys. Rev. Lett.* **125**, 252501 (2020).
- [22] M. Duer, T. Aumann, R. Gernher, V. Panin, S. Paschalis *et al.*, *Nature (London)* **606**, 678 (2022).

- [23] R. Lazauskas, E. Hiyama, and J. Carbonell, *Phys. Rev. Lett.* **130**, 102501 (2023).
- [24] K. Hagino, N. Takahashi, and H. Sagawa, *Phys. Rev. C* **77**, 054317 (2008).
- [25] T. Kubo, M. Ishihara, N. Inabe, H. Kumagai, I. Tanihata, K. Yoshida, T. Nakamura, H. Okuno, S. Shimoura, and K. Asahi, *Nucl. Instrum. Methods Phys. Res., Sect. B* **70**, 309 (1992).
- [26] Z. X. Cao, Y. L. Ye, J. Xiao, L. Lv, D. X. Jiang *et al.*, *Phys. Lett. B* **707**, 46 (2012).
- [27] J. Xiao, Y. L. Ye, Z. X. Cao, D. X. Jiang, T. Zheng *et al.*, *Chin. Phys. Lett.* **29**, 082501 (2012).
- [28] J. L. Lou, Y. L. Ye, D. Y. Pang, Z. X. Cao, D. X. Jiang, T. Zheng, H. Hua, Z. H. Li, X. Q. Li, Y. C. Ge *et al.*, *Phys. Rev. C* **83**, 034612 (2011).
- [29] See Supplemental Material at <http://link.aps.org/supplemental/10.1103/PhysRevLett.131.242501> for more details about the microscopic $\alpha + 4n$ model calculation, supplemental figures, and supplemental tables, which includes Ref. [30].
- [30] R. Imai, T. Tada, and M. Kimura, *Phys. Rev. C* **99**, 064327 (2019).
- [31] J. Wang, A. Galonsky, J. Kruse, P. Zecher, F. Deák, A. Horváth, A. Kiss, Z. Seres, K. Ieki, and Y. Iwata, *Nucl. Instrum. Methods Phys. Res., Sect. A* **397**, 380 (1997).
- [32] H. You, Y. Song, J. Xiao, and Y. Ye, *Plasma Sci. Technol.* **14**, 473 (2012).
- [33] S. W. Huang, Z. H. Yang, F. M. Marqués, N. L. Achouri, D. S. Ahn *et al.*, *Few-Body Syst.* **62**, 102 (2021).
- [34] S. Leblond, F. M. Marqués, J. Gibelin, N. A. Orr, Y. Kondo, T. Nakamura *et al.*, *Phys. Rev. Lett.* **121**, 262502 (2018).
- [35] A. Korshennikov and T. Kobayashi, *Nucl. Phys.* **A567**, 97 (1994).
- [36] T. Nilsson, F. Humbert, W. Schwab, H. Simon, M. Smedberg *et al.*, *Nucl. Phys.* **A598**, 418 (1996).
- [37] M. Zinser, F. Humbert, T. Nilsson, W. Schwab, H. Simon *et al.*, *Nucl. Phys.* **A619**, 151 (1997).
- [38] L. V. Grigorenko, J. S. Vaagen, and M. V. Zhukov, *Phys. Rev. C* **97**, 034605 (2018).
- [39] Z. H. Yang, Y. L. Ye, Z. H. Li, J. L. Lou, J. S. Wang, D. X. Jiang *et al.*, *Phys. Rev. Lett.* **112**, 162501 (2014).
- [40] V. Lapoux and N. Alamanos, *Eur. Phys. J. A* **51**, 91 (2015).
- [41] M. Itoh, H. Akimune, M. Fujiwara, U. Garg, N. Hashimoto, T. Kawabata *et al.*, *Phys. Rev. C* **84**, 054308 (2011).
- [42] I. J. Thompson, *Comput. Phys. Rep.* **7**, 167 (1988).
- [43] J. A. Tostevin, J. S. Al-Khalili, M. Zahar, M. Belbot, J. J. Kolata, K. Lamkin, D. J. Morrissey, B. M. Sherrill, M. Lewitowicz, and A. H. Wuosmaa, *Phys. Rev. C* **56**, R2929 (1997).
- [44] Z. H. Yang, Y. L. Ye, Z. H. Li, J. L. Lou, J. S. Wang, D. X. Jiang *et al.*, *Phys. Rev. C* **91**, 024304 (2015).
- [45] M. N. Harakeh and A. E. L. Dieperink, *Phys. Rev. C* **23**, 2329 (1981).
- [46] G. Satchler, *Nucl. Phys.* **A472**, 215 (1987).
- [47] B. Laurent, F. M. Marqués, C. Angulo, N. I. Ashwood, M. J. G. Borge *et al.*, *J. Phys. G* **46**, 03LT02 (2019).
- [48] W. von Oertzen, H. Bohlen, B. Gebauer, M. von Lucke-Petsch, A. Ostrowski *et al.*, *Nucl. Phys.* **A588**, c129 (1995).
- [49] K. Markenroth, M. Meister, B. Eberlein, D. Aleksandrov, T. Aumann *et al.*, *Nucl. Phys.* **A679**, 462 (2001).
- [50] M. Ito and K. Ikeda, *Rep. Prog. Phys.* **77**, 096301 (2014).
- [51] M. Kimura, T. Suhara, and Y. Kanada-En'yo, *Eur. Phys. J. A* **52**, 373 (2016).
- [52] G. R. Satchler and D. T. Khoa, *Phys. Rev. C* **55**, 285 (1997).
- [53] A. Ozawa, T. Suzuki, and I. Tanihata, *Nucl. Phys.* **A693**, 32 (2001), radioactive nuclear beams.
- [54] M. Zhukov, B. Danilin, D. Fedorov, J. Bang, I. Thompson, and J. Vaagen, *Phys. Rep.* **231**, 151 (1993).
- [55] S. M. Wang and W. Nazarewicz, *Phys. Rev. Lett.* **126**, 142501 (2021).
- [56] Y. T. Oganessian, V. I. Zagrebaev, and J. S. Vaagen, *Phys. Rev. Lett.* **82**, 4996 (1999).
- [57] K. Hagino and H. Sagawa, *Phys. Rev. C* **93**, 034330 (2016).
- [58] S. C. Pieper, R. B. Wiringa, and J. Carlson, *Phys. Rev. C* **70**, 054325 (2004).
- [59] B. Zhou, Y. Funaki, H. Horiuchi, Z. Ren, G. Röpke, P. Schuck, A. Tohsaki, C. Xu, and T. Yamada, *Phys. Rev. Lett.* **110**, 262501 (2013).
- [60] B. Zhou, Y. Funaki, H. Horiuchi, Z. Ren, G. Röpke, P. Schuck, A. Tohsaki, C. Xu, and T. Yamada, *Phys. Rev. C* **89**, 034319 (2014).
- [61] B. Zhou, *Prog. Theor. Exp. Phys.* **2018**, 041D01 (2018).
- [62] T. Myo, R. Ando, and K. Katō, *Phys. Lett. B* **691**, 150 (2010).